



**HAL**  
open science

## Metal-Only Reflect-Transmit-Array Unit Cell with Polarization-Dependent Performance

Ángel Palomares-Caballero, Carlos Molero, Juan F Valenzuela-Valdés, Pablo Padilla, María García-Vigueras, Raphaël Gillard

► **To cite this version:**

Ángel Palomares-Caballero, Carlos Molero, Juan F Valenzuela-Valdés, Pablo Padilla, María García-Vigueras, et al.. Metal-Only Reflect-Transmit-Array Unit Cell with Polarization-Dependent Performance. 2023 17th European Conference on Antennas and Propagation (EuCAP), Mar 2023, Florence, Italy. pp.1-5, 10.23919/EuCAP57121.2023.10133394 . hal-04571254

**HAL Id: hal-04571254**

**<https://hal.science/hal-04571254v1>**

Submitted on 7 May 2024

**HAL** is a multi-disciplinary open access archive for the deposit and dissemination of scientific research documents, whether they are published or not. The documents may come from teaching and research institutions in France or abroad, or from public or private research centers.

L'archive ouverte pluridisciplinaire **HAL**, est destinée au dépôt et à la diffusion de documents scientifiques de niveau recherche, publiés ou non, émanant des établissements d'enseignement et de recherche français ou étrangers, des laboratoires publics ou privés.

# Metal-Only Reflect-Transmit-Array Unit Cell with Polarization-Dependent Performance

Ángel Palomares-Caballero\*, Carlos Molero\*, Juan F. Valenzuela-Valdés\*, Pablo Padilla\*,  
María García-Vigueras†, Raphaël Gillard†

\*Departament of Signal Theory, Telematics and Communications, Universidad de Granada (CITIC-UGR),  
18071 Granada, Spain

†UMR CNRS 6164, INSA Rennes, IETR, 35708 Rennes, France  
*email: angelpc@ugr.es*

**Abstract**—A metal-only reflect-transmit-array unit cell whose operation is dependent on the incident polarization is presented. The proposed unit cell is based on 3D geometry which allows a high level of independent phase tuning for orthogonal and linear incident polarizations. In our unit cell, the horizontal polarization is reflected while the vertical polarization is transmitted. The modification of the reflected phase is done by the length of a metal block located at the end of the slits where the horizontal polarization propagates. The modification of the transmitted phase is changed by the depth of the corrugations implemented in the slit that supports the propagation of the vertical polarization. The results obtained in transmission mode show an impedance matching below -15 dB with a linear phase response from 30 GHz to 50 GHz. For the reflected polarization, there is almost total reflection with phase performance that is also linear along the frequency.

**Index Terms**—Metal-only, millimeter-waves, polarization control, reflect-transmit-array.

## I. INTRODUCTION

Reflectarrays and transmitarrays emerged as versatile antenna solutions to increase the directivity of a primary radiating source. Reflectarrays [1] provide the collimation of the incident wave towards the desired direction by reflection while the transmitarray [2] performs it in transmission. Recently, a new type of antenna array has been proposed that combines the performance of both a reflectarray and a transmitarray in the same physical structure. This new antenna design concept has been referred to as reflect-transmit-array (RTA) antenna [3]. Due to the behavior that allows this type of antenna array, the elements that form it must provide both transmission and reflection, both with a similar magnitude. Regarding the introduced phase by the RTA antenna, this also has a similar value in both reflection and transmission making equal the angles of reflection and transmission of the main beams [3]–[5]. This situation does not allow to select independently the main direction of radiation in both reflection and transmission. In view of this issue, some works have proposed some solutions such as using the array-sparse method [6] or using a unit cell with a different phase response in dual band [7]. Nevertheless, some disadvantages appear when employing the previous solutions which is that the aperture efficiency decreases

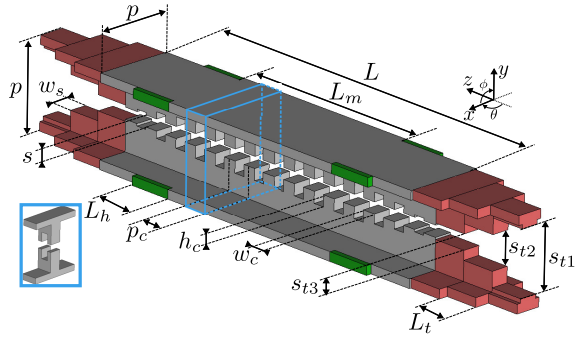
or that the desired performance is not in the same frequency band.

One manner to address these problems is that the reflection or transmission operation is each associated with a different polarization. That is, the RTA antenna should be polarization selective. In this way, the phase introduced in each orthogonal polarization can be independently tuned. Several RTA antennas based on this design strategy have been proposed for orthogonal linear polarizations [8]–[13]. In some of the previous works, this polarization-dependent behavior is achieved by stacking PCB layers where there is a pair of layers that are gratings in horizontal and vertical arrangement. There are also other works in the literature showing RTA antenna designs selective to orthogonal circular polarizations [14], [15].

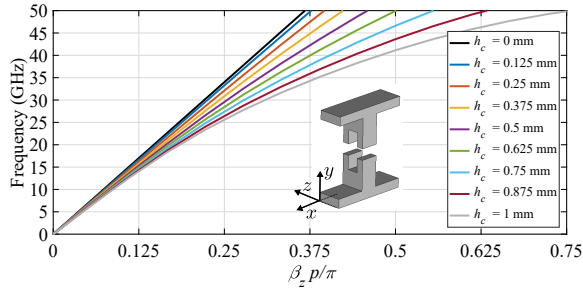
Up to now, the RTA designs with polarization-dependent performance presented in the literature need the use of dielectrics which leads to reduce the antenna efficiency, specially when the frequency increases. In this paper, a new approach to design a RTA antenna with only metal structures is presented. The proposed metal-only unit cell design has a 3D geometry to take advantage of the benefits offered by this kind of structures [16]. More specifically, the one that allows for an independent control of different impinging linear polarizations [17]. Up to now, using 3D unit cells, only radiofrequency devices in transmission as polarizers [17], [18] and transmitarrays [19], or in reflection as reflectarrays [20]–[22], have been reported. Here, the proposed metal-only unit cell allows an independent selection of the phase value introduced for transmission and reflection depending on the incoming linear polarization.

## II. PROPOSED RTA UNIT CELL

In Fig. 1(a), the metal-only RTA unit cell is illustrated. All the parts seen in this figure are metal, more specifically aluminum has been considered as the material for all the simulations in this work. For the electromagnetic (EM) analysis of the unit cell, a plane wave excitation in positive  $z$ -direction has been considered. When this incident wave has the electric field (E-field) in  $y$ -direction, it will be regarded as vertically polarized (V-



(a)

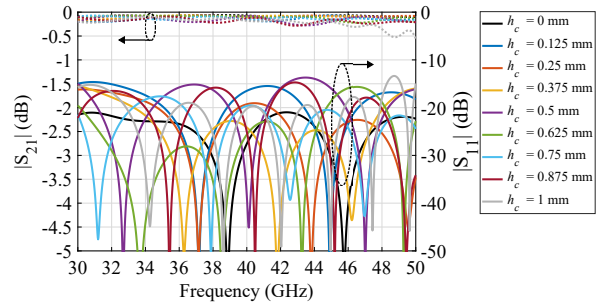


(b)

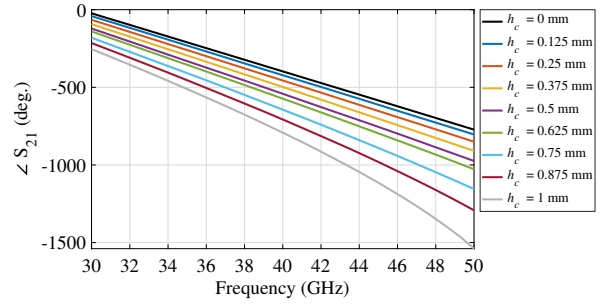
Fig. 1. (a) 3-D view of the proposed metal-only RTA unit cell. (b) Dispersion diagram of the corrugated unit cell. The dimensions (in mm) are:  $p = 4$ ,  $w_s = 0.8$ ,  $L = 17.2$ ,  $L_m = 9$ ,  $L_t = 1.55$ ,  $s_{t1} = 2.84$ ,  $s_{t2} = 1.49$ ,  $s_{t3} = 0.67$ ,  $s = 0.5$ ,  $p_c = 1.1$  and  $w_c = 0.5$ .

pol) while if it has the E-field in  $x$ -direction, it will be regarded as horizontally polarized (H-pol). In the EM analysis, the Frequency Solver of CST Studio Suite is employed where the periodic boundary conditions are set in the  $x$ - and  $y$ -directions of the unit cell. In a periodic environment, the unit cells are connected in the  $x$ -axis and they can be viewed as an array of parallel plate waveguides that are separated of a distance  $p$  in the  $x$ - and  $y$ -directions. The input port in the simulation is located in negative  $z$ -direction while the output port is placed in positive  $z$ -direction.

In order to better describe the unit cell, its most important parts have been highlighted in different colors in Fig. 1(a). The beginning and end of the structure (colored in red) are formed by three sections where each one of them corresponds to a slit with thickness  $w_s$  and width  $s_t$ . The length of these sections is  $L_t$  and the slits are aligned along both the  $x$ - and  $y$ - directions, they are symmetrical. These sections have been included to provide a good impedance matching between the free space and that of the slits located in the gray part. Following the characteristic impedance characterization procedure shown in [18], the impedance of these three sections has been designed to implement a binomial impedance transformer [23]. The block highlighted in green in Fig. 1(a) represents the phase tuning element for horizontal polarization. Depending on the  $L_h$  value, the reflected phase is modified. This part of the unit



(a)



(b)

Fig. 2. S-parameters when a V-pol wave impinges on the unit cell and the  $h_c$  is swept: (a) in magnitude and, (b) in phase.

cell design is based on [22]. The last part of the unit cell is highlighted in gray. This corresponds to a slit of thickness  $w_s$  and width  $s$ , which has implemented corrugations along its length  $L$ . Metal corrugations are a way to realize slow wave structures and therefore modify the phase of the wave propagating along them. Fig. 1(b) shows the dispersion diagram of the unit cell with corrugations. As it can be seen in this figure, by increasing the depth of the corrugation  $h_c$ , the phase constant  $\beta_z$  is modified producing a higher phase shift. In addition, the modification of the  $\beta_z$  preserves the linearity along the frequency which is beneficial for the design of broadband transmitarray. It is important to point out that at the beginning and at the end of the slit with corrugations, a taper in  $h_c$  of the corrugated unit cells is needed to keep the reflection level low. The value of  $L$  has been selected to cover the  $360^\circ$  phase shift at the center frequency.

#### A. Transmission and reflection performance

After detailing the structure of the proposed unit cell, this subsection presents the phase and magnitude performances in both reflection and transmission.

Fig. 2 shows the results in phase and magnitude when the incident wave is V-pol in case of normal incidence ( $\phi = 0^\circ$ ,  $\theta = 0^\circ$ ). It can be seen that the reflection coefficient  $|S_{11}|$  remains below -15 dB from 30 GHz to 50 GHz for all values of the range set for  $h_c$ . Consequently, the transmission coefficient  $|S_{21}|$  stays quite high, above -0.5 dB over the entire frequency band. In relation to the phase introduced in transmission [see

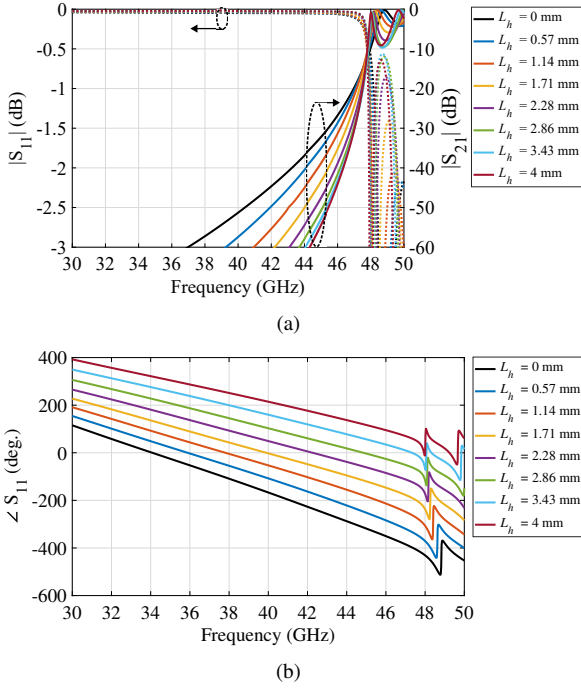


Fig. 3. S-parameters when a H-pol wave impinges on the unit cell and the  $h_c$  is swept: (a) in magnitude and, (b) in phase.

Fig. 2(b)], by modifying the value of  $h_c$ , the produced phase shift  $\angle S_{21}$  is tuned reaching a range of  $360^\circ$ . Moreover, as predicted from the dispersion diagram, the phase shift keeps a linear behavior over the frequency band. Cross polarization values have been omitted for the sake of conciseness but these are below  $-50$  dB across the whole band.

Regarding the reflection performance when an H-pol wave is impinging, the results are shown in Fig. 3. In this case, the tuning of the reflected phase is modified by the  $L_h$  value. The behavior of the  $|S_{11}|$  and  $|S_{21}|$  can be found in Fig. 3(a). It can be observed that there is almost total reflection up to about 47 GHz. From this frequency the  $|S_{21}|$  increases greatly. This is due to the separation between metal plates in the  $y$ -direction. This separation value allows the propagation of  $TE_{10}$  along the unit cell since its cutoff frequency for the  $p - w_s$  separation is 46.8 GHz. This problem has a straightforward solution by redesigning the unit cell to reduce the separation value and thus, increase the cutoff frequency of the undesired  $TE_{10}$  mode. In Fig. 3(b), it is shown the reflected phase value  $\angle S_{11}$  when  $L_h$  is swept. The reflected phase behavior over the frequency is also linear and covers the  $360^\circ$  of variation necessary for reflectarray design. At the end of the frequency band, this desired phase behavior deteriorates due to the undesired propagation of the  $TE_{10}$  mode.

In order to show that there is independence in the phase tuning of both incident linear polarizations, Fig. 4 is displayed. This shows the transmission phase along the

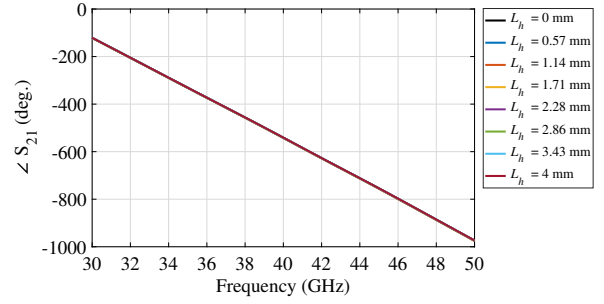


Fig. 4. Transmission phase in the vertical polarization when the length of the tuning elements  $L_h$  of the horizontal polarization is varied. The value for the depth of corrugation is fixed ( $h_c = 0.5$  mm) for all curves where  $L_h$  is swept.

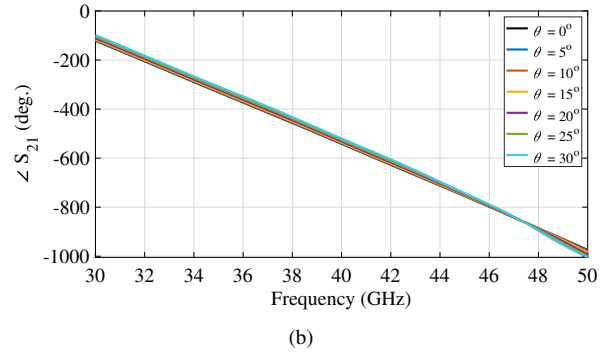
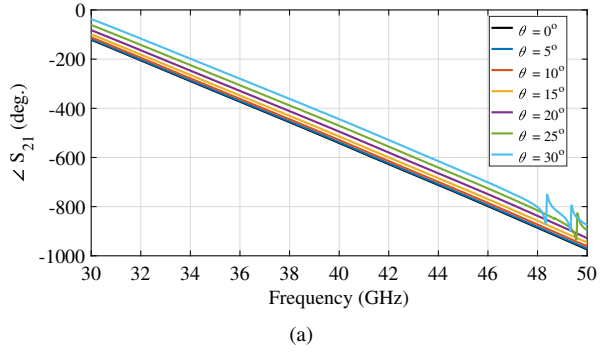


Fig. 5. Phase response for the V-pol under different oblique angles ( $\theta$ ) when  $h_c = 0.5$  mm. (a) In the H-plane. (b) In the E-plane.

frequency when the tuning parameter  $L_h$  for horizontal polarization is modified. It can be seen how there is no disturbance of the  $|S_{21}|$  curve, this is thanks to the 3D geometry used in the unit cell that allows a large decoupling between both orthogonal linear polarizations.

### B. Oblique Incidence Performance

This subsection presents the performance of the proposed unit cell in oblique incidence situations. For this purpose, it has been studied how the phase in transmission and reflection is modified when the angle of incidence  $\theta$  varies. The planes under study are the H-plane ( $XZ$  plane) and the E-plane ( $YZ$  plane). Fig. 5 displays the phase response along the frequency when a V-pol wave impinges and the  $\theta$  is modified. The

depth value  $h_c$  is fixed for all values of  $\theta$  and planes analyzed. When the value of  $\theta$  is varied, the phase value in transmission is also modified but in an acceptable manner and maintaining the desired linear behavior in the whole frequency band. Also, it can be noted how the oblique incidence on the E-plane is the one that produces the least modification in the transmitted phase. On the other hand, Fig. 6 shows the reflected phase response when the value of  $\theta$  changes. As in the previous case, the reflected phase is altered in an allowable manner while preserving linearity with frequency. Complementary to the previous polarization, for horizontal polarization, the H-plane is the most robust to changes in  $\theta$ .

### III. RTA FARFIELD RESULTS

Once the unit cell has been thoroughly analyzed, this section shows its application in a complete RTA antenna. For this purpose, the simulated farfields have been calculated for a RTA composed of  $21 \times 21$  unit cells illuminated by a standard WR22 horn with 20 dBi gain in oblique incidence ( $\phi = -90^\circ$ ,  $\theta = 20^\circ$ ). Fig. 7 shows the 3D radiation diagrams obtained when the array is illuminated with vertical and horizontal polarization. In the case of V-pol illumination, the phase map of the array has been computed to collimate the transmitted wave on the positive  $z$ -axis ( $\phi = 0^\circ$ ,  $\theta = 180^\circ$ ) as shown in Fig. 7(a). In contrast, for illumination with a H-pol wave, the collimation of the wave is done in reflection towards the direction: ( $\phi = 90^\circ$ ,  $\theta = 20^\circ$ ). This can be seen in Fig. 7(b). The resulting directivities produced by the RTA for both polarization situations are approximately 29.5 dBi.

### IV. CONCLUSION

In this paper, a metal-only unit cell design has been presented that enables transmission or reflection depending on the impinging linear polarization. Thanks to the 3D geometry of the proposed unit cell, the modification of the reflected and transmitted phases is performed independently. For phase tuning in reflection, the length of the metal block located in the slit that supports the propagation of the horizontal polarization is modified. For phase tuning in transmission, corrugations have been included along the slit that allow the propagation of vertical polarization. Depending on the depth of the corrugations, the value of the transmitted phase is tuned. For both reflection and transmission, the performance achieved is as desired with linear phase response from 30 GHz to 50 GHz covering a phase tuning range of  $360^\circ$ . The unit cell has also been analyzed for different angles at oblique incidence. The simulated results have shown a good performance in oblique incidence, maintaining the linear phase response up to approximately  $30^\circ$ . The proposed unit cell has been used in a complete RTA antenna design. The radiation pattern results obtained demonstrate the collimation of the incident wave into two different directions depending on the polarization used in the feeder. Furthermore, a substantial increase of

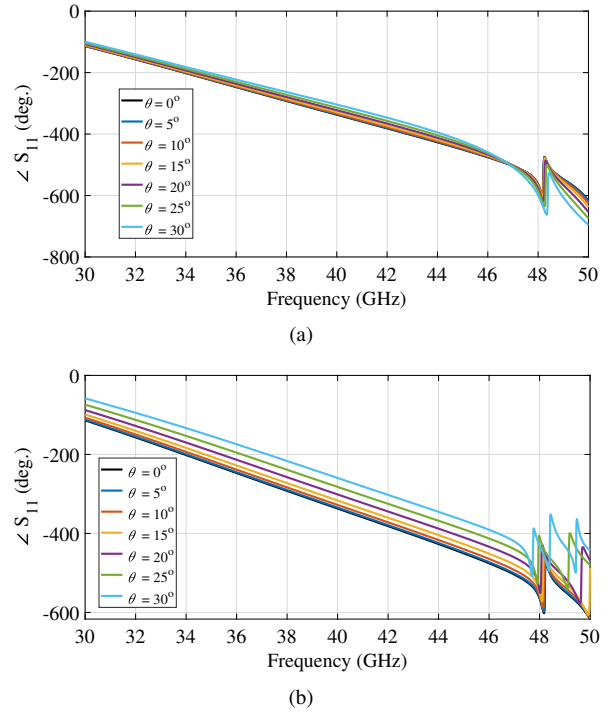


Fig. 6. Phase response for the H-pol under different oblique angles ( $\theta$ ) when  $L_h = 2$  mm. (a) In the H-plane. (b) In the E-plane.

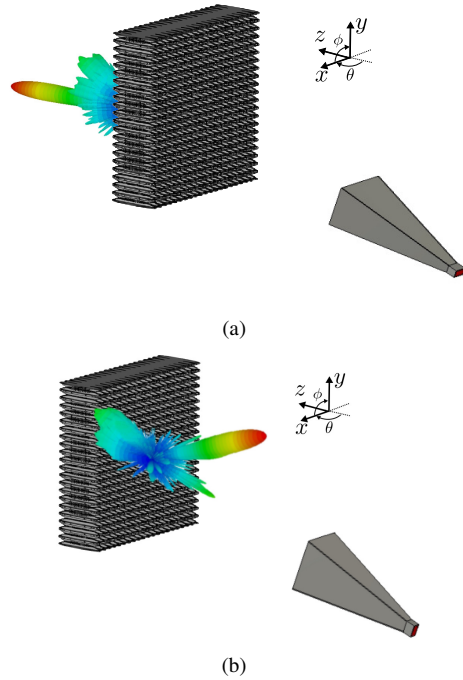


Fig. 7. Farfield results of the proposed RTA antenna at 40 GHz when it is illuminated by a: (a) V-pol wave and, (b) H-pol wave. The feeder is a standard WR22 horn antenna.

the incident wave directivity is observed in both polarization cases. The proposed design shows the capability of being metal-only and having a polarization-dependent behavior, which has not been presented before for RTAs.

## ACKNOWLEDGMENT

This work was supported in part by the Spanish Government under Project PID2020-112545RB-C54, Project RTI2018-102002-A-I00, Project TED2021-129938B-I00 and Project TED2021-131699B-I00; in part by the “Junta de Andalucía” under Project A-TIC-608-UGR20, Project PYC20-RE-012-UGR, and Project P18.RT.4830; and in part by the Predoctoral Grant FPU18/01965.

## REFERENCES

- [1] P. I. Theoharis, R. Raad, F. Tubbal, M. U. A. Khan and A. Jamalipour, “Wideband Reflectarrays for 5G/6G: A Survey,” *IEEE Open J. Antennas Propag.*, vol. 3, pp. 871-901, 2022.
- [2] J. R. Reis, M. Vala and R. F. S. Caldeirinha, “Review Paper on Transmitarray Antennas,” *IEEE Access*, vol. 7, pp. 94171-94188, 2019.
- [3] F. Yang, R. Deng, S. Xu, and M. Li, “Design and experiment of a near-zero-thickness high-gain transmit-reflect-array antenna using anisotropic metasurface,” *IEEE Trans. Antennas Propag.*, vol. 66, no. 6, pp. 2853–2861, Jun. 2018.
- [4] M. R. Akram, G. Ding, K. Chen, Y. Feng, and W. Zhu, “Ultrathin single layer metasurfaces with ultra-wideband operation for both transmission and reflection,” *Adv. Mat.*, vol. 32, no. 12, Mar. 2020, Art. no. 197308.
- [5] M. Wang, S. Xu, F. Yang and M. Li, “A 1-Bit Bidirectional Reconfigurable Transmit-Reflect-Array Using a Single-Layer Slot Element With PIN Diodes,” *IEEE Trans. Antennas Propag.*, vol. 67, no. 9, pp. 6205-6210, Sept. 2019.
- [6] S. L. Liu, X. Q. Lin, Y. H. Yan and Y. L. Fan, “Generation of a High-Gain Bidirectional Transmit-Reflect-Array Antenna With Asymmetric Beams Using Sparse-Array Method,” *IEEE Trans. Antennas Propag.*, vol. 69, no. 9, pp. 6087-6092, Sept. 2021.
- [7] X. Wang, J. Ding, B. Zheng, S. An, G. Zhai, and H. Zhang, “Simultaneous realization of anomalous reflection and transmission at two frequencies using bi-functional metasurfaces,” *Sci. Rep.*, vol. 8, p. 1876, Jan. 2018.
- [8] T. Cai, G. -M. Wang, X. -L. Fu, J. -G. Liang and Y. -Q. Zhuang, “High-Efficiency Metasurface With Polarization-Dependent Transmission and Reflection Properties for Both Reflectarray and Transmitarray,” *IEEE Trans. Antennas Propag.*, vol. 66, no. 6, pp. 3219-3224, June 2018.
- [9] W. Song *et al.*, “A Single-Layer Reflect-Transmit-Array Antenna With Polarization-Dependent Operation,” *IEEE Access*, vol. 9, pp. 167928-167935, 2021.
- [10] S. Liu and Q. Chen, “A Wideband, Multifunctional Reflect-Transmit-Array Antenna With Polarization-Dependent Operation,” *IEEE Trans. Antennas Propag.* vol. 69, no. 3, pp. 1383-1392, March 2021.
- [11] G. Shang *et al.*, “Transmission-Reflection-Integrated Multiplexed Janus Metasurface,” *ACS Appl. Electron. Mater.* vol. 3, no. 6, pp. 2638-2645, 2021.
- [12] H. Yi, S. -W. Qu, K. -B. Ng, C. K. Wong and C. H. Chan, “Terahertz Wavefront Control on Both Sides of the Cascaded Metasurfaces,” *IEEE Trans. Antennas Propag.*, vol. 66, no. 1, pp. 209-216, Jan. 2018.
- [13] Y. Wang *et al.*, “Broadband High-Efficiency Ultrathin Metasurfaces With Simultaneous Independent Control of Transmission and Reflection Amplitudes and Phases,” *IEEE Trans. Microw. Theory Tech.*, vol. 70, no. 1, pp. 254-263, Jan. 2022.
- [14] W. Yang, K. Chen and Y. Feng, “Multifunctional Metasurface for Broadband Reflect-Transmit-Array Antenna at 5G Millimeter-Wave Band,” in *2022 16th European Conference on Antennas and Propagation (EuCAP)*, 2022, pp. 1-5.
- [15] J. Feng *et al.*, “Reflect-Transmit-Array Antenna With Independent Dual- Circularly Polarized Beam Control,” *IEEE Antennas Wirel. Propag. Lett.*, 2022, doi: 10.1109/LAWP.2022.3202955.
- [16] A. Alex-Amor, Á. Palomares-Caballero and C. Molero, “3-D Metamaterials: Trends on Applied Designs, Computational Methods and Fabrication Techniques,” *Electronics*, vol. 11, no. 3, p. 410, Jan. 2022.
- [17] C. Molero Jimenez, E. Menargues and M. García-Vigueras, “All-Metal 3-D Frequency-Selective Surface With Versatile Dual-Band Polarization Conversion,” *IEEE Trans. Antennas Propag.*, vol. 68, no. 7, pp. 5431-5441, July 2020.
- [18] C. Molero, H. Legay, T. Pierré and M. García-Vigueras, “Broadband 3D-Printed Polarizer Based on Metallic Transverse Electromagnetic Unit-Cells,” *IEEE Trans. Antennas Propag.*, vol. 70, no. 6, pp. 4632-4644, June 2022.
- [19] X. Wang, Y. Cheng and Y. Dong, “Millimeter-Wave Dual-Polarized Metal Transmitarray Antenna With Wide Gain Bandwidth,” *IEEE Antennas Wirel. Propag. Lett.*, vol. 21, no. 2, pp. 381-385, Feb. 2022.
- [20] C. Molero *et al.*, “Metamaterial-Based Reconfigurable Intelligent Surface: 3D Meta-Atoms Controlled by Graphene Structures,” *IEEE Commun. Mag.*, vol. 59, no. 6, pp. 42-48, June 2021.
- [21] Á. Palomares-Caballero, C. Molero, P. Padilla, M. García-Vigueras and R. Gillard, “Metal-Only Reflectarray Unit Cell for Dual-Polarization Control,” in *2022 16th European Conference on Antennas and Propagation (EuCAP)*, 2022, pp. 1-4.
- [22] Á. Palomares-Caballero, C. Molero Jiménez, P. Padilla, M. García-Vigueras and R. Gillard, “Wideband 3-D-Printed Metal-only Reflectarray for Controlling Orthogonal Linear Polarizations,” to be appear in *IEEE Trans. Antennas Propag.*
- [23] D. Pozar, *Microwave Engineering*, 4th ed. Hoboken, NJ, USA: Wiley, 2004.